JCB Journal of Cell Biology

REPORT

# Calcineurin-dependent regulation of endocytosis by a plasma membrane ubiquitin ligase adaptor, Rcr1

Lu Zhu[1,2], Richa Sardana[1,2], Daniel K. Jin[1,2], and Scott D. Emr[1,2]

**Rsp5, the Nedd4 family member in yeast, is an E3 ubiquitin ligase involved in numerous cellular processes, many of which require Rsp5 to interact with PY-motif containing adaptor proteins. Here, we show that two paralogous transmembrane Rsp5 adaptors, Rcr1 and Rcr2, are sorted to distinct cellular locations: Rcr1 is a plasma membrane (PM) protein, whereas Rcr2 is sorted to the vacuole. Rcr2 is delivered to the vacuole using ubiquitin as a sorting signal. Rcr1 is delivered to the PM by the exomer complex using a newly uncovered PM sorting motif. Further, we show that Rcr1, but not Rcr2, is up-regulated via the calcineurin/Crz1 signaling pathway. Upon exogenous calcium treatment, Rcr1 ubiquitinates and down-regulates the chitin synthase Chs3. We propose that the PM-anchored Rsp5/Rcr1 ubiquitin ligase-adaptor complex can provide an acute response to degrade unwanted proteins under stress conditions, thereby maintaining cell integrity.**

## Introduction

The Rsp5/Nedd4 E3 ubiquitin ligase is responsible for the ubiquitination of membrane proteins, which serves as a sorting signal for endocytosis and lysosomal turnover. PY motifs (with a typical consensus sequence of P/L-P-x-Y) bind the WW domains of Rsp5/Nedd4 family members (Rotin and Kumar, 2009). Many Rsp5/Nedd4 substrates lack PYmotifs and must rely on interactions with adaptor proteins for ubiquitination and vacuolar sorting. Arrestin-related trafficking adaptors (ARTs) recruit Rsp5 to the PM to ubiquitinate PM proteins under certain conditions (Lin et al., 2008). Recently, membrane-anchored Rsp5 adaptors have also been characterized. Ssh4 and Ear1 are membrane-embedded adaptors that recruit Rsp5 to endosome and vacuole membranes, directing the ubiquitination of membrane proteins, which then enter the multivesicular body pathway via the ESCRT machinery for degradation (Léon et al., 2008; Li et al., 2015b; Sardana et al., 2019; Zhu et al., 2017). Overexpression of the membrane-embedded adaptors Ssh4 and Ear1 leads to Rsp5 accumulation at the endosome and vacuole membranes, respectively (Léon et al., 2008; Li et al., 2015b).

Multiple potential Rsp5 adaptor proteins were identified by proteomics (Gupta et al., 2007). After searching for other candidate Rsp5 adaptors, our attention was drawn to a pair of transmembrane proteins, Rcr1 and Rcr2. Based on sequence similarity, Rcr1 and Rcr2 were classified as small type-I transmembrane proteins with PY-motifs. Representative proteins in this family include Comm in *Drosophila*, PRRG4 in humans, and Rcr1/Rcr2 in yeast (Justice et al., 2017). Comm recruits Nedd4 to down-regulate the Robo receptor at the cell surface of axons, which is required for midline crossing (Myat et al., 2002). *RCR1*, but not *RCR2*, was identified as a multicopy suppressor in yeast for congo red or calcofluor white (CFW) sensitivity (Imai et al., 2005). *SSH4* and *RCR2/SSH5* were found as high copy suppressors for sulfonylurea (SU) sensitivity of *shr3*Δ mutants, and the *SSH* gene name is derived as suppressor of SHr3 deletion (Kota et al., 2007b). Later, *SSH4* and *RCR2* were isolated as high copy suppressors of the Ser/Thr protein phosphatase *ptc1*Δ mutant at alkaline pH (Tatjer et al., 2016). However, the function and regulation of Rcr proteins remain unknown.

In this study, we found that Rcr1 and Rcr2 are sorted to the PM and vacuole, respectively. We demonstrate that ubiquitin targets Rcr2 to the vacuole, and exomer sorts Rcr1 to the PM using a bipartite sorting motif (LxYYD and LxxPxxxVV) within the Rcr1 tail. Additionally, Rcr2 overexpression results in the down-regulation of some vacuole membrane proteins. We found that Rcr1 is up-regulated (>20 fold) by the calcineurin/Crz1 signaling pathway upon $Ca^{2+}$ treatment, which results in down-regulation of Chs3 by inducing its endocytosis and vacuolar degradation. The calcineurin signaling pathway regulates cell wall remodeling by transcriptional induction of *FKS2* (encoding a subunit of the cell wall β[1,3]-D-glucan synthase) upon pheromone, calcium signaling, or loss of *FKS1* (Garrett-Engele et al., 1995; Mazur et al., 1995). Here we have uncovered a novel role for the PM adaptor Rcr1 in regulating Chs3 PM abundance via the calcineurin/Crz1 signaling pathway.

[1]Weill Institute for Cell and Molecular Biology, Cornell University, Ithaca, NY; [2]Department of Molecular Biology and Genetics, Cornell University, Ithaca, NY.

Correspondence to Scott D. Emr: sde26@cornell.edu.

## Results and discussion

### Rcr1 and Rcr2 have distinct cellular localizations

Since Rcr1 and Rcr2 have PY-motifs in their cytosolic tails (Fig. 1 A and Fig. S1 A), we first confirmed that Rcr1 and Rcr2 interact with Rsp5. To test this, we performed co-immunoprecipitations (IPs) from cells expressing Rcr1-GFP or Rcr2-GFP and blotted for Rsp5. Indeed, endogenous Rsp5 binds to both Rcr1 and Rcr2. This interaction was abolished in the PY-motif mutants (Fig. 1 B).

We found that Rcr1-GFP localized to the PM (Fig. 1 C). Since *rcr1*Δ is mildly CFW sensitive (Imai et al., 2005), we confirmed that Rcr1-GFP was as functional as nontagged Rcr1 by testing cell growth on CFW (Fig. S1, B and C). However, Rcr1 was previously characterized as an ER membrane protein (Imai et al., 2005; Smoyer et al., 2016). To confirm that Rcr1 is not localized at the cortical ER, we examined its localization in an ER-PM tether mutant, in which the cortical ER is collapsed into the cytoplasm (Manford et al., 2012). Rcr1 was exclusively localized to PM, even in the ER-PM tether mutant (Fig. S1 D). In contrast to Rcr1, Rcr2-GFP was sorted to the vacuole, and the GFP signal in the vacuolar lumen is the result of the accumulation of free GFP when Rcr2-GFP is internalized into the lumen (Fig. 1 C). Rcr2-Myc was previously shown to be associated with the vacuole membrane (Kota et al., 2007a), but we hypothesized that proteolysis of the Myc tag by vacuolar proteases eliminated its vacuole lumen signal. Consistent with this, Rcr2-pHluorin exhibited a weak vacuole membrane signal in WT cells (the luminal pHluorin signal is quenched by the low pH, Fig. S1 E). We confirmed the functionality of Rcr2-GFP by its SU resistance in a *shr3*Δ mutant (Fig. S1, F and G). Together, these results establish that Rcr1 and Rcr2 have distinct cellular localizations.

Since Rcr1 and Rcr2 bind Rsp5, we next examined the recruitment of Rsp5 when overexpressing Rcr1 or Rcr2. Overexpression did not affect the sorting of Rcr1-GFP to the PM or Rcr2-GFP to the vacuole (Fig. S1 H). In WT cells, GFP-Rsp5 is diffuse in the cytosol and forms cytoplasmic puncta (Dunn et al., 2004; Fig. 1 D and Fig. S1 I). Upon Rcr2 overexpression, GFP-Rsp5 was recruited to the vacuole, and the cytosolic Rsp5 signal was reduced. Upon overexpressing Rcr1, Rsp5 was recruited to the PM (Fig. 1 D and Fig. S1 I). In addition, the membrane recruitment of Rsp5 was reduced to background levels in Rcr1 or Rcr2 PY-motif mutants (Fig. 1 D and Fig. S1 I). Together, these data demonstrate that Rcr1 and Rcr2 recruit Rsp5 to different cellular locations when they are overexpressed.

### Ubiquitin is a Golgi-to-endosome sorting signal

Based on the sequence similarity between these two proteins, we considered two possibilities for their distinct localizations. First, Rcr2 was sorted to the PM and then (unlike Rcr1) endocytosed and sorted to the vacuole. To test this, we analyzed Rcr2 localization in an endocytic mutant, *end3*Δ. The cell wall sensor protein Wsc1, which is continuously endocytosed and sorted to the vacuole (Piao et al., 2007), served as a control. In the *end3*Δ mutant, Wsc1-GFP was blocked at the PM, but the vacuolar sorting of Rcr2-GFP was unaffected (Fig. 1 E), which ruled out the possibility that Rcr2 was endocytosed. Biosynthetic transport of proteins to the vacuole proceeds via two pathways, the vacuolar protein sorting (VPS) or the AP-3 pathway (Burd et al., 1998). To test which pathway Rcr2 uses, we examined Rcr2-GFP localization in the AP-3 pathway mutant *apl5*Δ (Cowles et al., 1997a) and the VPS pathway mutant *vps45*Δ (Cowles et al., 1997b). In comparison with the classic AP-3 cargo protein GFP-ALP, Rcr2-GFP was not affected in *apl5*Δ. However, Rcr2-GFP was blocked in cytosolic punctate structures in a *vps45*Δ mutant (Fig. S1 J), suggesting that Rcr2 was sorted to the vacuole via the VPS pathway.

Rcr2 contains four lysines in its cytosolic domain, two of which have acidic residues nearby (KTE, 128–130; DKD, 146–148; Fig. S1 A), which are not present in Rcr1. Lysines with nearby acidic residues are more likely to be ubiquitinated (Radivojac et al., 2010), which may affect Rcr2 sorting. Since the Rcr2 PY-motifs interact with Rsp5, we examined if the Rsp5–Rcr2 interaction is required for vacuolar sorting. $Rcr2^{py1+2}$ sorted to both the PM and the vacuole in WT cells, whereas in the *end3*Δ mutant, it was blocked at the PM (Fig. 1 F), indicating Rcr2 requires Rsp5-mediated ubiquitination to sort to the endosome and vacuole. Consistently, mutating all cytosolic lysines to arginines ($Rcr2^{K/R}$) caused PM sorting (Fig. 1 F). In contrast, $Rcr1^{py1+2}$ still sorts to the PM (Fig. 1 G). These results suggest that ubiquitin serves as the Golgi-to-endosome sorting signal for Rcr2.

Additionally, adding lysines (EAA^KTE, 130–132; VNS^DKD, 148–150; Fig. S1 A) to Rcr1 induced its vacuolar sorting (Fig. 1 G). To ensure that Rsp5 is the major E3 ligase for Rcr2 ubiquitination, we examined Rcr2-GFP localization in a $rsp5^{ts}$ mutant (*rsp5-1*). At semi-permissive temperature, Rcr2 was largely rerouted to the PM (Fig. 1 H). Further, to validate that Rcr2 is ubiquitinated, we expressed $Rcr2^{WT}$ or $Rcr1^{+K}$ in a *doa4*Δ (deubiquitination defective) mutant to stabilize ubiquitinated membrane proteins after multivesicular body sorting. After IP, ubiquitinated species of $Rcr2^{WT}$ and $Rcr1^{+K}$ were detected (Fig. 1 I).

We next investigated the possible functions of Rcr2. Since Rcr2 overexpression recruited Rsp5 to the vacuole, we hypothesized that vacuolar membrane proteins may be down-regulated upon Rcr2 overexpression. To test this, we used Wsc1-acLL-GFP (WaG), an artificial cargo protein routed to the vacuolar membrane via an acidic-dileucine motif that is recognized by AP-3 adaptor protein. WaG is ubiquitinated and sorted to the vacuole lumen in an Ssh4-dependent manner (Sardana et al., 2019). In an *ssh4*Δ mutant, WaG was sorted to the vacuole lumen when Rcr2 or $Rcr1^{+K}$ were overexpressed (Fig. 1 J; and Fig. S2, A and B), but not $Rcr2^{py1+2}$ (Fig. S2, C and D). Other vacuolar membrane proteins (Ypq1, Avt3, Avt4, and Vba4) were also sorted to the vacuolar lumen upon Rcr2 overexpression (Fig. S2 E). Gap1 was shown to have altered activity at the surface in an Rcr1/Rcr2-dependent manner (Kota et al., 2007b). As shown in the Fig. S2 F, no significant vacuole lumen signal of Gap1 was observed, suggesting that Gap1 is not a direct cargo for Rcr2 or Rcr1. These results indicate that recruitment of Rsp5 to the vacuole membrane by Rcr2 induces vacuole membrane proteins turnover, and suggests that Rcr2 may also function as a Rsp5 adaptor on the vacuole membrane, although its native cargo proteins and the conditions that result in their degradation require further investigation.

### Exomer sorts Rcr1 to the PM

Exomer is the only known vesicle coat mediating TGN-to-PM trafficking in yeast (Spang, 2015). Exomer contains five

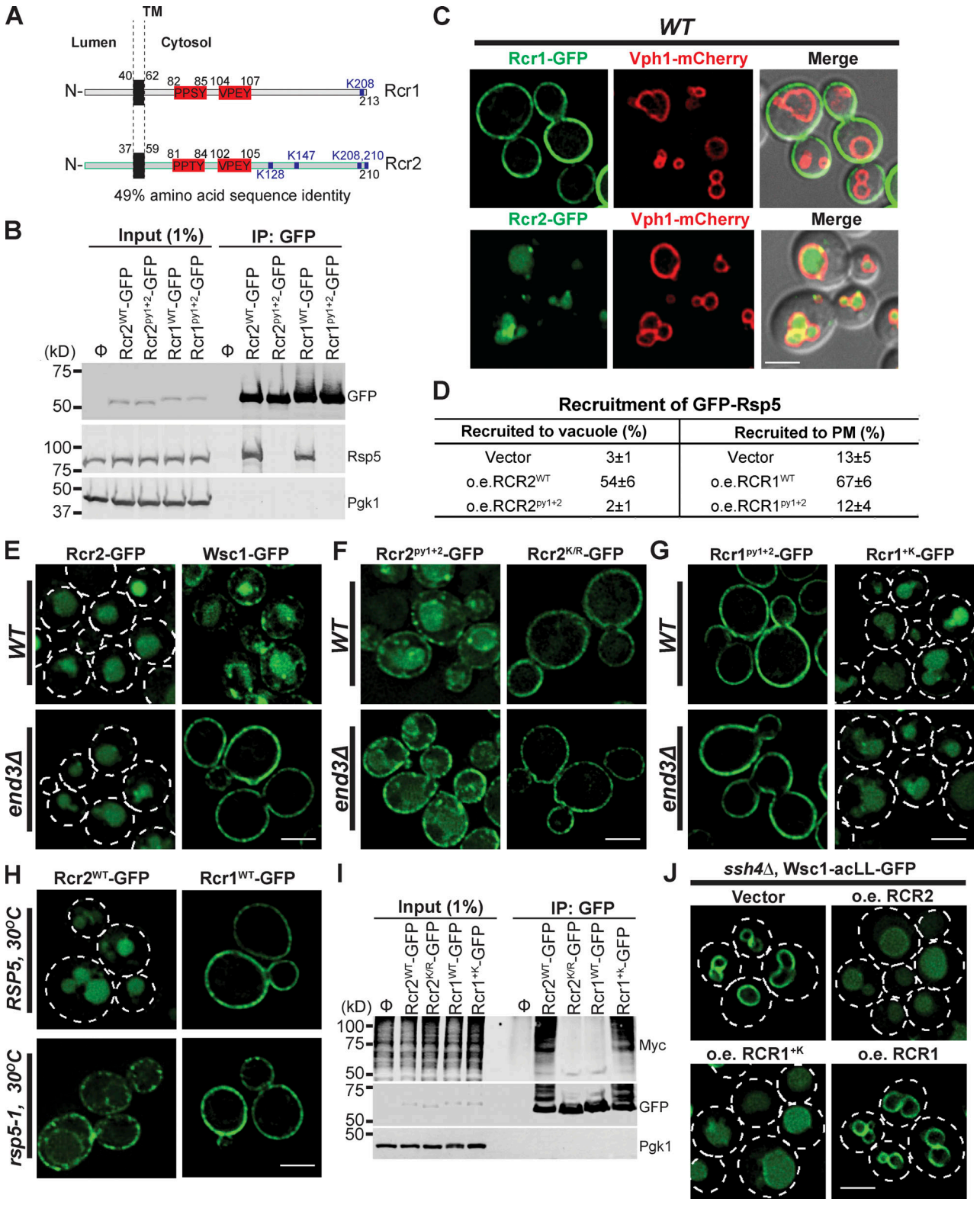


Figure 1. **The paralogous transmembrane proteins Rcr1 and Rcr2 have distinct cellular localizations, and ubiquitin is a Golgi-to-endosome sorting signal for Rcr2. (A)** Schematic of Rcr1 and Rcr2 in yeast strain SEY6210. **(B)** IP of Rcr1 and Rcr2 WT and PY-motif mutants. **(C)** Localization of Rcr1-GFP and Rcr2-GFP by fluorescence microscopy. Vph1-mCherry marks the vacuole membrane. **(D)** GFP-Rsp5 recruitment to the vacuole or PM upon overexpression of RCR1 or RCR2. Representative images are shown in Fig. S1 I. The ratio of GFP-Rsp5 recruitment to PM or vacuole was measured from $n$ = 20 cells. **(E)** Fluorescence microscopy of Rcr2-GFP and Wsc1-GFP localization in WT and *end3*Δ. **(F)** $Rcr2^{py1+2}$ and $Rcr2^{K/R}$ localization in WT and *end3*Δ. **(G)** $Rcr1^{py1+2}$ and $Rcr1^{+K}$ localization in WT and *end3*Δ. **(H)** Rcr2-GFP and Rcr1-GFP localization in *RSP5* and *rsp5-1* grown at semi-permissive temperature (30°C). **(I)** IP of the indicated proteins in *doa4*Δ expressing Myc-Ub (Ubiquitin). **(J)** WaG localization in *ssh4*Δ, with *RCR2*, $RCR1^{+K}$, or *RCR1* overexpression. Scale bars, 2 µm.

subunits: the core coat protein Chs5 and four paralogous Chs5-Arf1 binding proteins: Chs6, Bch2, Bch1, and Bud7. PM sorting signals in most exomer-dependent cargos remain unidentified (Anton et al., 2017; Ritz et al., 2014; Weiskoff and Fromme, 2014); the motif in Fus1 was identified, but it cannot sort a foreign protein to the PM in an exomer-dependent manner (Barfield et al., 2009). To test if Rcr1 requires exomer for its PM delivery, we expressed Rcr1-GFP in *chs5*Δ and *bud7*Δ*bch1*Δ, and found that it mis-sorted to the vacuole membrane (Fig. 2 A and Fig. S3 A). To determine if vacuole membrane Rcr1 resulted from endocytosis, we used *chs5*Δ*end3*Δ and found that Rcr1 is partially mis-sorted to vacuole (Fig. S3 B). These results show that efficient sorting of Rcr1 to the PM requires exomer function. A portion of Rcr1 is still trafficked to the PM in exomer mutants, indicating that an alternative exomer-independent sorting pathway, likely a general secretion pathway for PM proteins, may traffic some Rcr1.

We next mapped the PM targeting sequence in Rcr1. Rcr1 with a truncated C terminus (Rcr1(ΔC])-GFP) sorts to the vacuole membrane, suggesting that the cytoplasmic tail contains PM targeting signals (Fig. S3 C). We generated a series of deletions in the Rcr1 cytosolic tail and screened for mutants that mis-sorted to the vacuole. We quantified the ratio of each Rcr1 mutant mis-sorted to vacuole membrane relative to the total amount of Rcr1 per cell and then converted it to "PM sorting defect score of Rcr1 by exomer" as described in Materials and methods. Removing residues 110–129 or 130–171 mis-sorted Rcr1 (Fig. 2 B and Fig. S3 D). We then performed alanine scanning within this region (Fig. S3, E and F), and found three Rcr1 regions that had defects in PM sorting: 115–120, 151–155, and 156–160 (Fig. 2 C). We mutated single amino acids to alanine within these patches, and found two motifs required for PM sorting: LxYYD and LxxPxxxVV (Fig. 2 D and Fig. S3 G). Further sequence analysis revealed that this bipartite sorting motif is highly conserved in Rcr1 and Rcr2 in different fungal species (Fig. 2, E and F).

To test if these sorting motifs are sufficient to target non-PM proteins to the PM, we made chimeras linking the N terminus and transmembrane domain of Vps10, a vacuole membrane protein, to the Rcr1 cytosolic tail (Vps10(ΔC)-Rcr1-GFP; Fig. S3 H). Vps10(ΔC)-GFP localized to the vacuole membrane (Fig. S3 I; Arlt et al., 2015). Interestingly, Vps10(ΔC)-Rcr1-GFP was partially sorted to the PM. Consistent with Rcr1 sorting, exomer is required for the PM targeting of this chimeric protein (Fig. 2 G; and Fig. S3, H and I), suggesting that the PM sorting motifs of Rcr1 are sufficient for exomer-dependent PM transport.

To see if the Rcr1 cytosolic tail is required for exomer binding, we examined the interaction between the Rcr1 C-terminal tail mutants and Chs5 using yeast two-hybrid and co-IP. Indeed, mutating 115–120 and 151–155 reduced the interaction between the Rcr1 cytosolic tail and Chs5 (Fig. 2 H and Fig. S3 J), indicating that these two regions are required for the Rcr1-Chs5 interaction, directly or indirectly.

We searched the yeast proteome for other proteins containing the LxxPxxxVV motif, and a weak match was found in the cytosolic tail of Fus1. The IxTPK motif is required for exomer-dependent sorting of Fus1 (Barfield et al., 2009). To make sure the mis-sorted Fus1 is not due to endocytosis, we confirmed that Fus1 is sorted to the shmoo tip in *end3*Δ and mis-sorted to vacuole in *chs5*Δ*end3*Δ with α-factor treatment (Fig. S3 K). Mutating single amino acids within the IxTPK patch and its downstream region revealed that Fus1 PM sorting was abolished in I176A and P199A mutants, whereas the Fus1 PM sorting exhibited mild defects in V183A and K184A (Fig. 2 I and Fig. S3 L), which indicates Fus1 has an exomer sorting motif (IxxPxxxVK), similar to the motif in Rcr1.

### Calcineurin/Crz1 signaling pathway regulates Rcr1 expression

We demonstrated that Rcr1 and Rcr2 were sorted to the PM and vacuole using different sorting signals (Fig. 2 J). We next investigated the regulation of Rcr1 expression and function. Previously, genome-wide studies (Marton et al., 1998; Yoshimoto et al., 2002) showed *RCR1* transcriptional up-regulation via the calcineurin signaling pathway. Consistently, Rcr1-GFP expression was highly induced by $Ca^{2+}$ treatment (Fig. 3, A and B). After $Ca^{2+}$ induction, Rcr1 is mainly sorted to the PM (Fig. 3 C) with some intracellular puncta. In contrast, $Ca^{2+}$ treatment does not affect the levels of Rcr2-GFP (Fig. 3 A), suggesting that the Rcr2 and Rcr1 have distinct transcriptional regulatory mechanisms.

In yeast, environmental stress increases intracellular $Ca^{2+}$ levels, which activates calmodulin and leads to the activation of calcineurin phosphatase (Cyert, 2003; Rusnak and Mertz, 2000). Activated calcineurin dephosphorylates several targets to promote cell survival, including the transcription factor Crz1 (Stathopoulos and Cyert, 1997), which binds to calcineurin-dependent response elements (Yoshimoto et al., 2002). To see if Rcr1 induction requires the calcineurin signaling pathway, we examined Rcr1 levels in *crz1*Δ or *cnb1*Δ mutants (*CNB1* encodes the calcineurin regulatory B subunit; Cyert and Thorner, 1992), and found that Rcr1 up-regulation was completely abolished in these mutants (Fig. 3 D). The calcineurin pathway inhibitor FK506 also blocked Rcr1 up-regulation (Fig. 3 E). In Fig. 3 F, we showed that Rcr1 induction does not require the osmoregulatory mitogen-activated protein (MAP) kinase Hog1 signaling pathway. Thus, Rcr1 is up-regulated via the calcineurin/Crz1 signaling pathway.

We set out to test if $Ca^{2+}$ treatment affects Rsp5 recruitment by Rcr1. Co-IPs showed that more Rsp5 is recruited to Rcr1 with $Ca^{2+}$ treatment (Fig. 3 G). To ensure that this enhanced Rsp5 recruitment does not cause aberrant PM protein endocytosis, we examined the endocytosis of Mup1 after $Ca^{2+}$ treatment. Mup1 remains at the PM despite increased Rsp5 on the PM, and the endocytosis rate of the Mup1 induced by methionine does not change (Fig. 3, H and I). In line with this, overexpression of Rcr1 does not cause Mup1 vacuolar sorting (Fig. 3 J). It was reported that adaptor protein overexpression interferes with other non-cognate Rsp5-dependent processes (MacDonald et al., 2020). We therefore asked if the Rsp5 pool is depleted due to enhanced Rsp5 recruitment to Rcr1. We measured Rsp5 binding with the adaptor Art1, but the interaction between Rsp5 and Art1 is unaffected by $Ca^{2+}$ treatment (Fig. 3 K). Further, the PM $Ca^{2+}$ channels Mid1, Cch1, and Ecm7 were not degraded upon $Ca^{2+}$ treatment (Fig. 3, L–N).

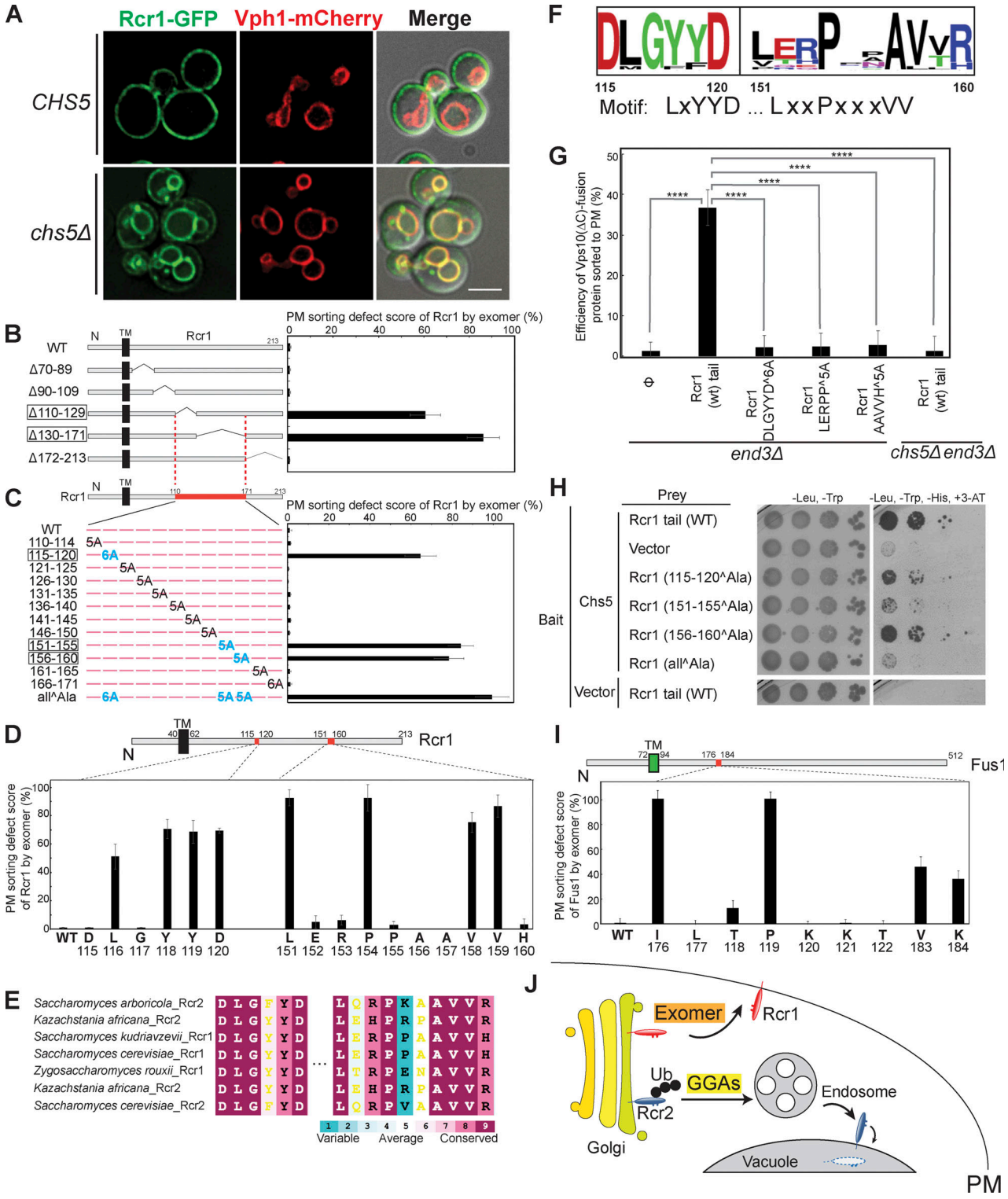


Figure 2. **Exomer sorts Rcr1 to the PM. (A)** Rcr1-GFP localization in WT and *chs5*Δ. Vph1-mCherry marks the vacuole membrane. Scale bar, 2 µm. **(B)** Left: Schematic of the tested Rcr1-GFP cytosolic tail deletions. Right: PM sorting defect score of Rcr1 by exomer (%). **(C)** Left: Schematic of the tested Rcr1 tail alanine scan mutants. Right: PM sorting defect score of Rcr1 by exomer (%). **(D)** Top: Schematic of the tested single alanine mutants. Bottom: PM sorting defect score of Rcr1 by exomer (%). **(E and F)** Conservation and weblogo analysis of regions 115–120 and 151–160 in the Rcr1 tail. **(G)** Percentage of Vps10(ΔC)-fusion proteins sorted to PM, analyzed by two-tailed *t* test. $P < 0.0001$, $n = 20$ cells. **(H)** Yeast two-hybrid analysis to detect the interaction between the bait Chs5 (residues 1–261) and prey Rcr1 tail mutants. Cells were spotted on the indicated synthetic growth media and incubated at 30°C for 3 d. **(I)** Top: Schematic of the tested single alanine mutants in Fus1. Bottom: PM sorting defect score of Fus1 by exomer (%). **(J)** Model for Rcr1 and Rcr2 sorting to different locations. Representative images for B, C, D, G, and I are shown in Fig. S3, D, F, G, I, and L, respectively.

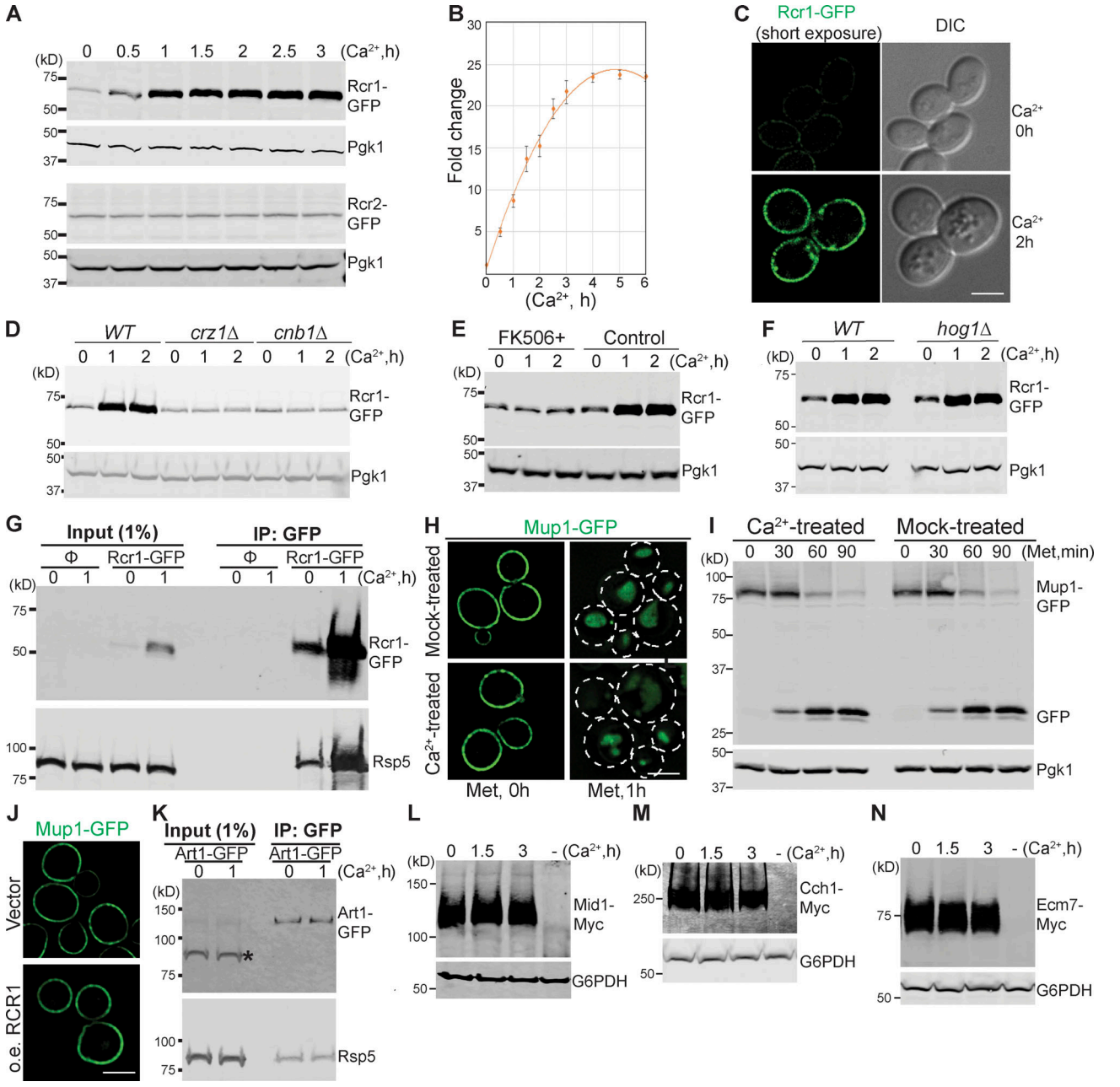


Figure 3. **Rcr1 is up-regulated via the calcineurin/Crz1 signaling pathway. (A)** Rcr1-GFP and Rcr2-GFP expression with 200 mM $CaCl_2$ treatment for the indicated times. **(B)** Quantification of Rcr1-GFP protein levels after $Ca^{2+}$ treatment in A. Fold change = Rcr1 after $Ca^{2+}$ treatment / Rcr1 before $Ca^{2+}$ treatment. *n* = 3. **(C)** Fluorescence microscopy of Rcr1-GFP and differential interference contrast (DIC) images before and after 2 h of $Ca^{2+}$ treatment using a short exposure. **(D)** Rcr1-GFP expression in WT, *crz1*Δ, and *cnb1*Δ cells after 200 mM $CaCl_2$ treatment. **(E)** Rcr1-GFP expression after treatment with 2 µM FK506 (LC Laboratories) for 60 min before 200 mM $CaCl_2$ treatment. Cells were collected at 0, 1, and 2 h after $CaCl_2$ treatment. **(F)** Rcr1-GFP expression in WT, *hog1*Δ cells after 200 mM $CaCl_2$ treatment. **(G)** IP of Rcr1-GFP after 1 h $Ca^{2+}$ treatment, and blotting for Rsp5. **(H)** Fluorescence microscopy of Mup1-GFP in WT cells. After mock- or 200 mM $Ca^{2+}$-treatment for 1 h, cells were treated with 20 µM methionine (Met) for 1 h. **(I)** Western blot analysis of Mup1-GFP in WT cells after Met treatment with or without calcium pre-treatment. After mock-treatment or 200 mM $Ca^{2+}$ treatment for 1 h, cells were treated with 20 µM Met for 0, 30, 60, and 90 min. **(J)** Fluorescence microscopy of Mup1-GFP in cells overexpressing *RCR1*. **(K)** IP of Art1-GFP after 1 h $Ca^{2+}$ treatment, and blotting for Rsp5. *A nonspecific protein band. **(L, M, and N)** Expression of Mid1-myc, Cch1-myc, and Ecm7-myc after 200 mM $Ca^{2+}$ treatment, 0, 1.5, and 3 h. Scale bars, 2 µm.

### Chs3 is sorted to the vacuole upon $Ca^{2+}$ treatment

It was shown that Rcr1 up-regulation gave rise to resistance to CFW (Imai et al., 2005). We observed that the overexpression of either $RCR1^{WT}$ or $RCR2^{K/R}$ gives rise to CFW resistance in WT cells (Fig. 4 A). Since Chs3 produces over 90% of the chitin in the yeast cell wall (Bulawa, 1992; Shaw et al., 1991), we hypothesized that Chs3 is degraded with Rcr1 overexpression. As anticipated, Chs3 sorts to the vacuole for degradation with overexpression of *RCR1*, but not *RCR2* or *SSH4* (Fig. 4, B–D), and this is blocked with $Rcr1^{py1+2}$ overexpression, demonstrating Rsp5 dependence (Fig. 4, E–G).

We next examined the Chs3 sorting in WT and *rcr1*Δ after $Ca^{2+}$ treatment. In WT cells, Chs3 is initially localized at the

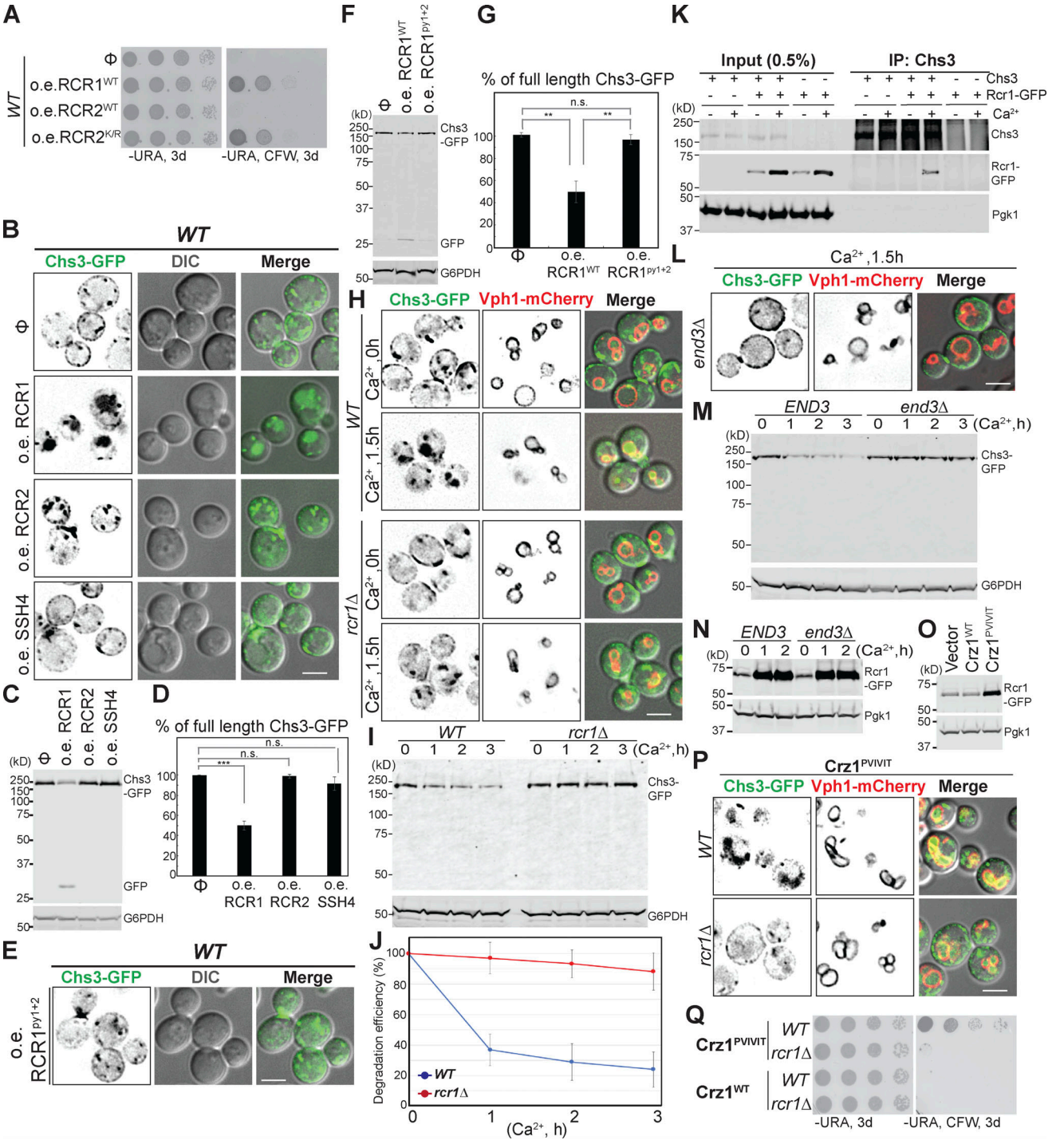


Figure 4. **Chs3 is sorted to the vacuole upon $Ca^{2+}$ treatment. (A)** Strains overexpressing *RCR1*, *RCR2*, or *RCR2*$^{K/R}$ were spotted on synthetic media ± 150 µg/ml CFW. **(B)** Chs3-GFP localization in cells overexpressing *RCR1*, *RCR2*, or *SSH4*. **(C)** Chs3-GFP degradation in cells overexpressing *RCR1*, *RCR2*, or *SSH4*. **(D)** Quantification of full-length Chs3-GFP in C, *n* = 3. **(E)** Chs3-GFP localization in cells overexpressing *RCR1*$^{py1+2}$. **(F)** Chs3-GFP degradation in cells overexpressing *RCR1* or *RCR1*$^{py1+2}$. **(G)** Quantification of full-length Chs3-GFP in F. **(H)** Chs3-GFP localization WT and *rcr1*Δ before (0 h) and after (1.5 h) 200 mM $Ca^{2+}$ treatment. Vph1-mCherry labels the vacuole membrane. **(I)** Chs3-GFP degradation in WT and *rcr1*Δ cells after 200 mM $Ca^{2+}$ treatment for the indicated times. **(J)** Quantification of Chs3-GFP degradation efficiency in F, *n* = 3. **(K)** Rcr1-GFP IP after 200 mM $Ca^{2+}$ treatment, blotting for co-IPed Chs3. **(L)** Chs3-GFP localization in *end3*Δ after 200 mM $Ca^{2+}$ treatment. **(M)** Chs3-GFP degradation in WT or *end3*Δ after 200 mM $Ca^{2+}$ for the indicated times. **(N)** Rcr1-GFP expression in WT and *end3*Δ after 200 mM $Ca^{2+}$ for the indicated times. **(O)** Rcr1-GFP expression in cells with WT Crz1 or Crz1$^{PVIVIT}$. **(P)** Chs3-GFP localization in WT or *rcr1*Δ expressing Crz1$^{PVIVIT}$. **(Q)** *crz1*Δ and *crz1*Δ*rcr1*Δ cells expressing WT Crz1 or Crz1$^{PVIVIT}$ spotted on synthetic media ± 200 µg/ml CFW. Scale bars, 2 µm.

bud-neck and the PM then sorted to the vacuole, and this sorting and degradation is reduced in *rcr1*Δ (Fig. 4, H–J), demonstrating that Chs3 vacuolar sorting upon $Ca^{2+}$ treatment requires Rcr1. To further show that Rcr1 functions as a Rsp5 adaptor, we examined the interaction between Rcr1 and Chs3. A small fraction of Rcr1-GFP co-IPed Chs3, but only after $Ca^{2+}$ treatment (Fig. 4 K), suggesting that the activation of Rcr1 via the calcineurin/Crz1 pathway is required for its adaptor function. Chs3 vacuolar sorting is due to endocytosis, since Chs3 remains at the PM in an *end3*Δ mutant (Fig. 4, L and M), despite normal $Ca^{2+}$ Rcr1 induction (Fig. 4 N).

Since the calcineurin pathway triggers Rcr1 up-regulation, we anticipated that $Ca^{2+}$ treatment will cause CFW resistance. However, $Ca^{2+}$ and CFW form a precipitate, preventing us from carrying out this experiment. The calcineurin-docking site of Crz1, PxIxIT, can be altered to PVIVIT ($Crz1^{PVIVIT}$) to increase its affinity for calcineurin and resulting in hyperactivity (Roy et al., 2007). As predicted, $Crz1^{PVIVIT}$ increases Rcr1 levels approximately eightfold (Fig. 4 O). Consistently, Chs3 sorted to the vacuole with $Crz1^{PVIVIT}$ in a Rcr1-dependent manner (Fig. 4 P), and CFW resistance increased (Fig. 4 Q), suggesting that the calcineurin/Crz1 signaling pathway regulates Chs3 at the PM via Rcr1 up-regulation.

### Rcr1-Rsp5 is required for Chs3 ubiquitination at the PM

To test if Chs3 undergoes ubiquitination upon $Ca^{2+}$ treatment, we IPed Chs3-GFP in *doa4*Δ while expressing Myc-Ub. After $Ca^{2+}$ treatment, the ubiquitinated species of Chs3-GFP can be detected (Fig. 5 A).

Since Rcr1 interacts with Rsp5, we confirmed that Chs3 degradation is delayed with $Rcr1^{py1+2}$ (Fig. 5, B–D), indicating that the interaction between Rcr1 and Rsp5 is required for Chs3 turnover upon $Ca^{2+}$ treatment. We next asked if Rsp5 is required for Chs3 ubiquitination upon $Ca^{2+}$ treatment. Using *rsp5-1,* at nonpermissive temperature (37°C) Chs3 remained at the PM, whereas its vacuole sorting and degradation was normal in WT at 37°C (Fig. 5, E–G), indicating that Rsp5 ubiquitinates Chs3, causing its endocytosis and vacuolar sorting.

In this study, we showed that Rcr2 is delivered to the vacuole using ubiquitin as a sorting signal. At the Golgi, the Golgi-located, gamma ear–containing, ARF-binding (GGA) family of coat proteins binds ubiquitinated membrane proteins and facilitate the incorporation of proteins into clathrin-coated vesicles destined for transport from the TGN to the endosome (Lauwers et al., 2009; Scott et al., 2004). Rcr2 contains a similar PM sorting signal as Rcr1, as evidenced by its PM sorting when ubiquitination is impaired, indicating that Rcr2 ubiquitination serves as the dominant targeting signal. One possible model that could explain this is that GGAs may have a higher affinity than the exomer for cargoes, or they may bind cargoes earlier in the Golgi than exomer. Consequently, Golgi-to-endosome targeting directed by ubiquitin overrides PM targeting.

Similar to Rcr1, transcription of *FKS2* is highly induced by exogenous $Ca^{2+}$ via the calcineurin signaling pathway (Mazur et al., 1995; Stathopoulos and Cyert, 1997). Why do yeast cells remodel the cell wall composition upon stimulation of the calcineurin signaling pathway? We reason that this is due to the compensatory effect between chitin and β(1,3)-D-glucan biosynthesis—the yin and yang of the yeast cell wall (Levin, 2005; Munro, 2013). β(1,3)-D-glucan is responsible for cell wall rigidity (Cid et al., 1995; Klis, 1994), whereas chitin maintains cell wall plasticity (Tharanathan and Kittur, 2003). $Ca^{2+}$ treatment gives rise to increased β(1,3)-D-glucan content (Luo et al., 2019). Remodeling these two cell wall components has been an adaptive response necessary to counterbalance cell wall stress (Cid et al., 1995; Klis, 1994). After calcineurin activation by $Ca^{2+}$ stress, yeast cells redistribute chitin and β(1,3)-D-glucan in the cell wall by up-regulation of Fks2 (to increase β[1,3]-D-glucan synthesis) and Rcr1 (to down-regulate chitin synthase Chs3).

Rcr1 and Rcr2 exhibit distinct cellular localization and transcriptional regulation. Overexpression of *RCR2* results in down-regulation of vacuolar membrane proteins, whereas overexpression (or up-regulation) of *RCR1* causes endocytosis and down-regulation of Chs3. These divergent results are in line with the recruitment of Rsp5 to distinct locations by overexpression of these adaptors (Fig. S1 I). How could Rcr1 recognize cargo proteins? We suggest two possible models for the Rcr1-Chs3 interaction upon $Ca^{2+}$ treatment. First, Rcr1-Rsp5 is up-regulated at the PM above a key threshold to ubiquitinate the Chs3 in its vicinity. Second, Chs3 may undergo conformational changes so that Rcr1-Rsp5 can recognize specific motifs of Chs3. In addition to $Ca^{2+}$, there are several cellular stimuli that induce the calcineurin pathway, such as high pH, $Na^{+}$, or $Mn^{2+}$ (Stie and Fox, 2008). We therefore believe that additional Rcr1-dependent cargo proteins at the PM will be identified.

In summary, our findings demonstrate that the Rcr1-Rsp5 complex regulates Chs3 abundance by ubiquitination, which results in its endocytosis. Instead of being recycled from the endosome to TGN by retromer, ubiquitinated Chs3 is delivered to the vacuole lumen upon $Ca^{2+}$ stress (Fig. 5 H). The existence of this ubiquitin-dependent PM protein down-regulation system provides an acute response to degrade unwanted proteins under stress conditions, thereby maintaining cell integrity.

## Materials and methods

### Yeast strains, plasmids, and cell growth conditions

The *RCR1*, *RCR2*, and *FUS1* genes were cloned from yeast strain SEY6210. The yeast strains bearing N-terminally GFP-tagged *AVT3* and *AVT4* were made by homologous recombination. The Ypq1-GFP and Vba4-GFP–expressing yeast strains were from laboratory stock (Li et al., 2015a,b). The yeast strains K1619 (W303-1A, ECM7-MYC::TRP), K1643 (W303-1A, CCH1-MYC::TRP), and K1659 (W303-1A, MID1-MYC::KAN) were generous gifts from the laboratory of K. Cunningham (Johns Hopkins University, Baltimore, MD). These tagged $Ca^{2+}$ channels coding genes with selection markers were PCR-amplified and transformed into yeast strain SEY6210.1. When necessary, additional gene deletion and tagging were made using a gene replacement technique with PCR-amplified cassettes (Longtine et al., 1998). All yeast strains and plasmids are described in Table S1 (Strains and plasmids). For fluorescent microscopy experiments, cells were grown overnight to mid-log phase (OD 600~0.5) in synthetic media at 30°C. For $Ca^{2+}$ stimulation experiments, cells were grown in synthetic media (yeast nitrogen base, dextrose, $NH_4Cl$, and necessary amino acids) to log phase (OD 600~0.8),

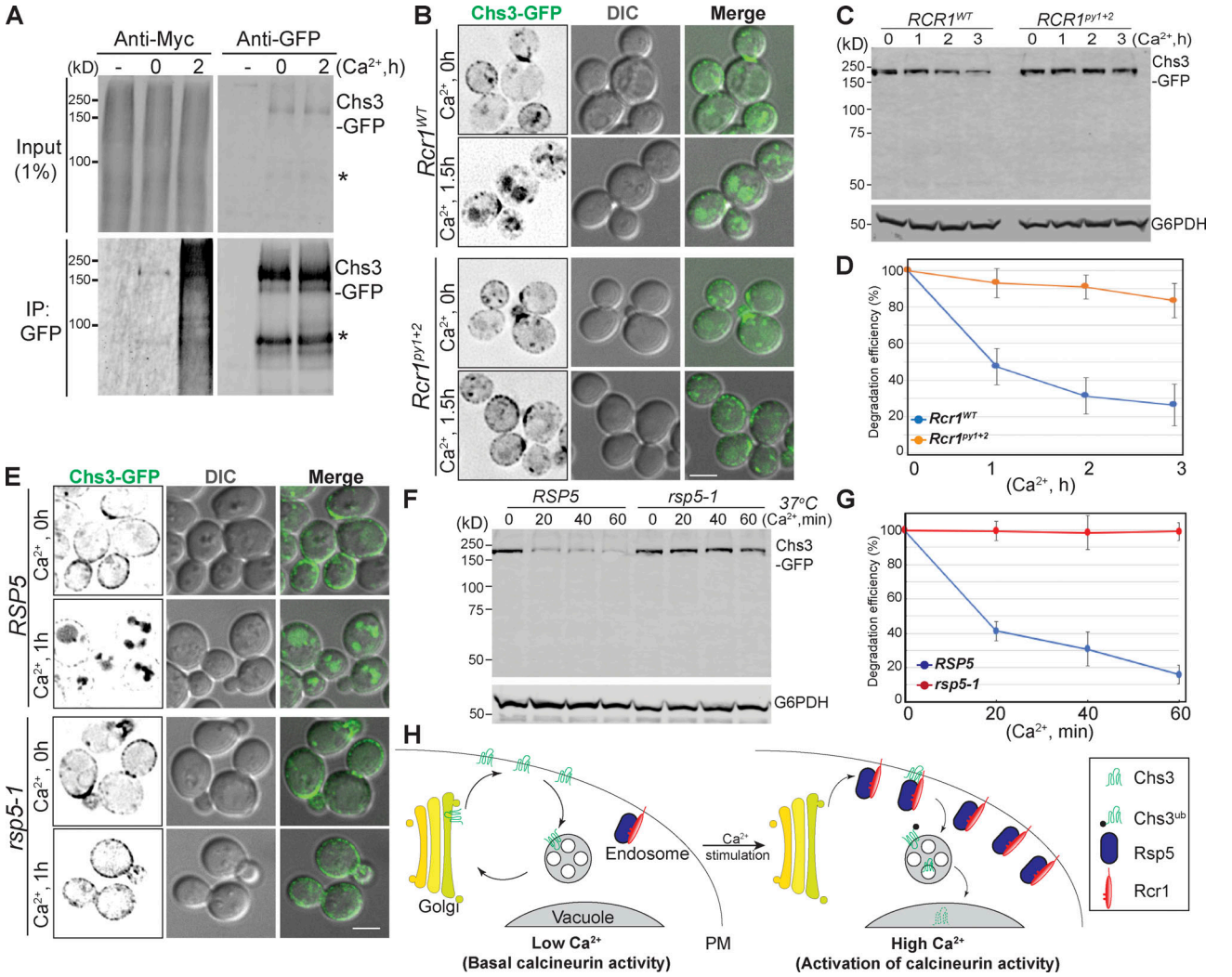


Figure 5. **Vacuolar sorting of Chs3 with $Ca^{2+}$ treatment is ubiquitination-dependent. (A)** IP of Chs3-GFP from *doa4Δpep4Δ* cells expressing Myc-Ub. The asterisks represent a Chs3-GFP fragment band. **(B)** Fluorescence microscopy of Chs3-GFP in cells expressing $Rcr1^{WT}$ or $Rcr1^{py1+2}$ after $Ca^{2+}$ treatment. **(C)** Chs3-GFP degradation in cells expressing $Rcr1^{WT}$ or $Rcr1^{py1+2}$ after 200 mM $Ca^{2+}$ treatment for the indicated times. **(D)** Quantification of Chs3-GFP degradation efficiency (%) in C, *n* = 3. **(E)** Fluorescence microscopy analysis of Chs3-GFP in *RSP5* and *rsp5-1* after preheating to 37°C for 15 min and treating with 200 mM $Ca^{2+}$. Images were obtained before (0 min) and after (30 min) $Ca^{2+}$ treatment at 37°C. Scale bars, 2 µm. **(F)** Chs3-GFP degradation in *RSP5* and *rsp5-1* mutant after preheating to 37°C for 15 min and treating with 200 mM $Ca^{2+}$ for the indicated times. **(G)** The quantification of Chs3-GFP degradation efficiency (%) in F, *n* = 3. **(H)** Model depicting ubiquitination-mediated endocytosis of Chs3 upon $Ca^{2+}$ treatment condition. In the presence of basal calcineurin activity, Chs3 undergoes constitutive protein endocytosis, recycling, and secretion via the PM-endosome-Golgi routes. With exogenous $Ca^{2+}$ treatment, calcineurin activity is enhanced and Rcr1 is up-regulated. Thereafter, more Rsp5 was recruited to PM so that Chs3 is ubiquitinated and exits the protein retrograde trafficking, then sorts to vacuole via the VPS pathway.

then treated with $CaCl_2$ (final concentration, 200 mM). For FK506 (LC Laboratories, dissolved in DMSO) with $Ca^{2+}$ treatment, cells were grown in synthetic media to log phase (OD 600~0.8), then treated with FK506 (final concentration, 1 mM) for 1 h before $Ca^{2+}$ treatment. For α-factor pheromone treatment, cells were grown in synthetic media to log phase (OD 600~0.4) and treated with 50 ng/ml α-factor pheromone peptide (Zymo Research) for 90 min, fixed with 3.7% formaldehyde (Thermo Fisher Scientific), and washed with water twice before imaging.

### CFW growth assay

Yeast strains were grown in appropriate medium to log phase (OD 600~0.8). 4 OD of cells were spun down and washed with sterilized water twice, then resuspended with 1ml of water. 10-fold dilutions of cells (starting from 4 OD/ml) were spotted onto synthetic growth medium plate (with selection if necessary) containing 150~200 µg/ml of CFW (Sigma-Aldrich, Fluorescent Brightener 28, Synonym: Calcofluor White). The plates were incubated at 30°C for 3–4 d. Sensitivity to CFW was determined by comparing the extent of colony density between strains on the control plate and the plates containing CFW.

### SU growth assay

Yeast mutant *shr3Δ* harboring different plasmids was cultured in synthetic dextrose medium to log phase (OD 600~0.8). 4 OD of cells were spun down and washed with sterilized water twice,

then resuspended with 1 ml water. 10-fold dilutions of cells (starting from 4 OD/ml) were spotted onto a Yeast Extract–Peptone–Dextrose (YPD) agar plate containing 100 µg/ml of sulfonylurea (2-[[[[(4-Methoxy-6-methyl-1,3,5-triazin-2-liter)amino] carbonyl]amino]sulfonyl] benzoic acid methyl ester, Quali-Pro Incorporation). The plates were incubated at 30°C for 3–4 d. Sensitivity to SU is determined by comparing the extent of colony density on the control plate and the plates containing SU.

### Fluorescence microscopy assay

For fluorescence microscopy, cells expressing GFP, pHluorin, or mCherry proteins were visualized using a DeltaVision Elite system (GE), equipped with a Photometrics CoolSnap HQ2/sCMOS Camera, a 100× objective, and a DeltaVision Elite Standard Filter Set ("FITC" for GFP/pHluorin fusion protein and "mCherry" for mCherry fusion proteins). Image acquisition and deconvolution were performed using Softworx.

### Whole cell lysate extraction and Western blotting

Whole cell extracts were prepared by incubating 6 ODs of cells in 10% trichloroacetic acid on ice for 1 h. Extracts were fully resuspended with ice-cold acetone twice by sonication, then vacuum dried. Dry pellets were mechanically lysed (3×, 5 min) with 100 µl glass beads and 100 µl Urea-Cracking buffer (50 mM Tris-HCl, pH 7.5, 8 M urea, 2% SDS, and 1 mM EDTA). 100 µl protein 2× sample buffer (150 mM Tris-HCl, pH 6.8, 7 M urea, 10% SDS, 24% glycerol, and bromophenol blue) supplemented with 10% 2-mercaptoethanol was added, and samples were vortexed for 5 min. The protein samples were resolved on 11% (m/v) SDS-PAGE gels and then transferred to nitrocellulose blotting membranes (GE Healthcare Life Sciences).

The following antibodies and dilutions were used in this study: rabbit polyclonal anti-G6PDH (1:30,000; SAB2100871; Sigma-Aldrich), mouse monoclonal anti-Pgk1 (1:20,000; 459250; Invitrogen), rabbit polyclonal anti-GFP (1:10,000; TP401; Torrypines), mouse monoclonal anti-GFP (1:1,000; B-2, sc-9996; Santa Cruz), mouse monoclonal anti-Myc (1:5,000, sc-40, Santa Cruz), Chs3 antiserum (generous gift from C. Fromme, Cornell University, Ithaca, NY), IRDye 800CW goat anti-mouse (1:10,000; 926–32210; LI-COR), IRDye 800CW goat anti-rabbit (1:10,000; 926–32211; LI-COR), IRDye 680LT goat anti-rabbit (1:10,000; 926–68021; LI-COR), and IRDye 680LT goat anti-mouse (1:10,000; 925–68070; LI-COR).

### Yeast two-hybrid analysis

The yeast two-hybrid strain HF7C (Feilotter et al., 1994) was co-transformed with pGADGH (empty vector or pGADGH-RCR1 mutants) and pGBT9 (empty vector or pGBT9-CHS5 [1–261]). Cells were grown to saturation in synthetic growth media (-Leu,-Trp) and 10-fold dilutions were spotted on synthetic growth media (-Leu,-Trp) and synthetic growth media (-Leu,-Trp,-His) supplemented with 2 mM 3-amino-1,2,4-triazole. The plates were incubated at 30°C for 3–4 d.

### IP assay

To examine the interaction between Rsp5 and Rcr1, Rcr2, or Art1, yeast strain GOY24 (lacking vacuolar hydrolase Pep4 and Prb1) bearing vector control, Rcr1-GFP, Rcr2-GFP, or Art1-GFP expression vectors were cultured in minimal media and grown to mid-log stage. 100 ODs of cells were collected and washed with water at 4°C. To examine the interaction between Chs3 and Rcr1-GFP, yeast strains GOY24, LZY1390, and LZY1533 were cultured in minimal media (using $NH_4Cl$ as a nitrogen source) and grown to mid-log phase. 150 ODs of cells were collected before and after 200 mM of $CaCl_2$ treatment and resuspended with ice-cold water three times. The cells were lysed in 500 µl of IP buffer (20 mM Tris-HCl, pH 7.5, 0.5 mM EDTA, pH 8.0, 0.5 mM EGTA, 0.5 mM NaF, 150 mM NaCl, 10% glycerol, 1 mM PMSF, 10 mM N-ethylmaleimide, and 1× Roche cOmplete Protease Inhibitor Tablet/50 ml). Cell extracts were prepared by glass-bead beating with 0.5-mm zirconia beads for five cycles of 30 s vortexing with 1 min breaks on ice. Membrane proteins were solubilized by adding 500 µl of 1% Triton X-100 in IP buffer. The lysates were incubated at 4°C for 30 min with rotation, then spun at 500 *g* for 5 min at 4°C. The supernatant was clarified by centrifugation at 16,000 *g* for 10 min. To detect the interaction between Rsp5 and adaptor proteins, the cleared lysate was incubated with GFP-nanotrap resin for 2 h at 4°C. To examine the interaction between Chs3 and Rcr1, the cleared lysate was prebound with 25 µl of protein-G Sepharose resin (GE Healthcare, 17–0885-01) at 4°C for 1 h with rotation, and the supernatant was incubated with 10 µl of Chs3 antiserum and 25 µl of protein-G Sepharose resin at 4°C for 3 h with rotation. After incubation, the resin was washed five times with 0.1% Triton X-100 in IP buffer, and the bound protein was eluted by 2× sample buffer and resolved on 11% (m/v) SDS-PAGE gels.

To examine the interaction between Chs5 and Rcr1 mutants, yeast strain LZY1506 bearing vector control or Rcr1-GFP mutants expression vectors were cultured in minimal media and grown to mid-log stage. 150 ODs of cells were collected and washed with water at 4°C. The cells were lysed in 500 µl of IP buffer (50 mM Hepes-KOH, pH 7.5, 2 mM MgOAc, 1 mM $CaCl_2$, 150 mM KOAc, 15% glycerol, and 1× Roche cOmplete Protease Inhibitor Tablet/50 ml). Cell extracts were prepared and membrane proteins were solubilized as above. The lysates were incubated with 2 mM DSP (Dithiobis(succinimidyl propionate), Thermo Fisher Scientific) for 2 h on ice and then mixed with 50 mM Tris-HCl (pH 7.5) for 15 min to stop the cross-linking reaction. To detect the Chs5 and Rcr1 protein interaction, the cleared lysate was incubated with GFP-nanotrap resin for 2 h at 4°C. After incubation, the resin was washed five times with 0.1% Triton X-100 in IP buffer, and the bound protein was eluted by 50 µl of 2× sample buffer and resolved on 11% (m/v) SDS-PAGE gels.

To examine the ubiquitination of Chs3 and Rcr proteins, Cells were grown to early log phase in synthetic media. Yeast strain (*doa4Δpep4Δ*) bearing Myc-Ub expression vector (Zhu et al., 2017) was induced with 100 µM $CuSO_4$ for 4 h before $Ca^{2+}$ treatment. 100 ODs of cells were harvested after 2 h $Ca^{2+}$ treatment and washed once with water at 4°C. The pellets were resuspended with 500 µl IP buffer (50 mM Hepes-KOH, pH 6.8, 150 mM KOAc, 2 mM MgOAc, 1 mM $CaCl_2$, 15% glycerol, and 1× Roche cOmplete Protease Inhibitor Tablet/50 ml). Cell extracts were prepared by adding 500 µl glass beads and beating for 30 s

(five cycles) with a 1-min break at 4°C. Membrane proteins were solubilized by adding 500 µl of 2% Triton X-100 in IP buffer. Cell lysates were clarified by spinning at 16,000 *g* for 10 min at 4°C. The resulting lysate was then incubated with 20 µl GFP-nanotrap resin for 4 h at 4°C. The resin was washed five times with 0.1% Triton X-100 in IP buffer. Bound protein was eluted by 50 µl of 2× sample buffer and resolved on 7% (m/v) SDS-PAGE gels.

### Quantification and statistical analysis of PM sorting defect score of Rcr1 and Fus1 by exomer

Yeast strains (WT, *end3*Δ mutant, or *chs5*Δ*end3*Δ mutant) harboring Rcr1-GFP or Fus1-GFP mutants vector were cultured in selection synthetic medium to mid-log phase (OD 600~0.5) at 30°C. Images of Rcr1-GFP and Fus1-GFP were taken by fluorescence microscopy. The fluorescence densities of Rcr1-GFP and Fus1-GFP sorted to PM or vacuole were selected and quantified using ImageJ. The corrected total fluorescence of each selection = selected density − (selected area × mean fluorescence of background readings). The ratio of Rcr1-GFP or Fus1-GFP mis-sorted to vacuole = (the corrected fluorescence density of Rcr1-GFP or Fus1-GFP localized at vacuole) / (the corrected fluorescence density of total Rcr1-GFP or Fus1-GFP). For each set of experiments, the ratio of WT Rcr1-GFP or Fus1-GFP mis-sorted to vacuole membrane in the *chs5*Δ*end3*Δ was used as a positive control, as shown in Fig. S3, B and K. For each Rcr1 and Fus1 mutant, the PM sorting defect score of Rcr1 by exomer (%) = (the ratio of Rcr1-GFP or Fus1-GFP mutant mis-sorted to vacuole in *end3*Δ mutant) / (the ratio of WT Rcr1-GFP or Fus1-GFP mis-sorted to vacuole in *chs5*Δ*end3*Δ mutant). In all figures, the average PM sorting defect score of Rcr1 and Fus1 by exomer from $n$ = 20 cells is shown for each mutant.

### *Quantification of efficiency of Vps10(ΔC)-Rcr1 fusion protein sorted to PM*

For each Vps10(ΔC)-Rcr1 fusion protein, yeast strains (*end3*Δ mutant or *chs5*Δ*end3*Δ mutant) harboring Vps10(ΔC)-Rcr1 mutants vector were cultured in selection synthetic medium to mid-log phase (OD 600~0.5) at 30°C. Image of Vps10(ΔC)-Rcr1 were taken by fluorescence microscopy. The Vps10(ΔC)-Rcr1 sorted to plasma membrane and the whole Vps10(ΔC)-Rcr1 per cell were selected and measured using ImageJ. The corrected total fluorescence of Vps10(ΔC)-Rcr1 in each selection = selected density − (selected area × mean fluorescence of background readings). The efficiency of Vps10(ΔC)-Rcr1 sorted to PM = (the corrected fluorescence density of Vps10(ΔC)-Rcr1 localized at PM) / (the corrected fluorescence density of total Vps10(ΔC)-Rcr1). In Fig. 2 G, the average efficiency of Vps10(ΔC)-Rcr1 fusion protein sorted to PM is shown for each mutant. The significance was determined using a two-tailed $t$ test, P value < 0.0001, α = 0.05 (Bonferroni correction), $n$ = 20 cells for each fusion protein.

### *Quantification of Rsp5 recruitment to PM or vacuole membrane*

Yeast strain (*leu2*::pRS305-GFP-Rsp5, Vph1-mCherry::*TRP*) harboring empty vector or vectors for overexpression of $RCR2^{WT}$, $RCR2^{py1+2}$, $RCR1^{WT}$, or $RCR1^{py1+2}$ was cultured in selection synthetic medium to mid-log phase (OD 600~0.5) at 30°C. Images of GFP-Rsp5 were taken by fluorescence microscopy. The GFP-Rsp5 signal at PM and vacuole were selected and measured by ImageJ. The corrected total fluorescence of each selection = selected density − (selected area × mean fluorescence of background readings). The ratio of GFP-Rsp5 recruitment to PM or vacuole = (the corrected fluorescence density of GFP-Rsp5 localized at PM or vacuole) / (the corrected fluorescence density of total GFP-Rsp5). In Fig. 1 D, the ratios of Rsp5 recruitment were measured from $n$ = 20 cells.

### *Quantification of Western blot band intensity*

All the Western blots in Fig. 3 A; Fig. 4, C, F, and I; Fig. 5, C and F; and Fig. S2, A and C, were quantified using ImageJ software. The significance for Fig. 4, D and G; and Fig. S2, B and D, was determined by two-tailed $t$ test, α = 0.05 (Bonferroni correction), $n$ = 3. For all figures, n.s. indicates not significant; *, P < 0.05; **, P < 0.01; ***, P < 0.001.

### Online supplemental material

Fig. S1 shows that recruitment of Rsp5 to different subcellular localizations by Rcr1 and Rcr2. Fig. S2 shows down-regulation of vacuole membrane proteins upon Rcr2 overexpression. Fig. S3 shows the plasma membrane sorting signal within the Rcr1 cytosolic tail. Table S1 is a list of yeast strains and yeast expression plasmids used in this study.

## Acknowledgments

We thank Dr. Chris Fromme (Cornell University, Ithaca, NY) for reagents, strains, plasmids and helpful advice. We appreciate Dr. Kyle Cunningham (Johns Hopkins University, Baltimore, MD) for providing us yeast strains. We are grateful to Dr. Matthew G. Baile, Dr. Mike Henne, Dr. Jeff Jorgensen, Dr. Sudeep Banjade, and Dr. Sho Suzuki for critical reading of the manuscript. We also thank other members of the Emr laboratory for helpful discussions.

The authors declare no competing interests.

Author contributions: L. Zhu designed and performed most the experiments, created the figures, and wrote the manuscript. R. Sardana developed methods and provided yeast strains. D.K. Jin contributed at an early stage of the project by performing some experiments. S.D. Emr supervised the project and edited the manuscript.

Submitted: 27 September 2019
Revised: 16 February 2020
Accepted: 28 April 2020

## References

Anton, C., B. Zanolari, I. Arcones, C. Wang, J.M. Mulet, A. Spang, and C. Roncero. 2017. Involvement of the exomer complex in the polarized transport of Ena1 required for *Saccharomyces cerevisiae* survival against toxic cations. *Mol. Biol. Cell.* 28:3672–3685. https://doi.org/10.1091/mbc.e17-09-0549

Arlt, H., F. Reggiori, and C. Ungermann. 2015. Retromer and the dynamin Vps1 cooperate in the retrieval of transmembrane proteins from vacuoles. *J. Cell Sci.* 128:645–655. https://doi.org/10.1242/jcs.132720

Barfield, R.M., J.C. Fromme, and R. Schekman. 2009. The exomer coat complex transports Fus1p to the plasma membrane via a novel plasma

membrane sorting signal in yeast. *Mol. Biol. Cell.* 20:4985–4996. https://doi.org/10.1091/mbc.e09-04-0324

Bulawa, C.E.. 1992. CSD2, CSD3, and CSD4, genes required for chitin synthesis in Saccharomyces cerevisiae: the CSD2 gene product is related to chitin synthases and to developmentally regulated proteins in Rhizobium species and Xenopus laevis. *Mol. Cell. Biol.* 12:1764–1776. https://doi.org/10.1128/MCB.12.4.1764

Burd, C.G., M. Babst, and S.D. Emr. 1998. Novel pathways, membrane coats and PI kinase regulation in yeast lysosomal trafficking. *Semin. Cell Dev. Biol.* 9:527–533. https://doi.org/10.1006/scdb.1998.0255

Cid, V.J., A. Durán, F. del Rey, M.P. Snyder, C. Nombela, and M. Sánchez. 1995. Molecular basis of cell integrity and morphogenesis in Saccharomyces cerevisiae. *Microbiol. Rev.* 59:345–386. https://doi.org/10.1128/MMBR.59.3.345-386.1995

Cowles, C.R., G. Odorizzi, G.S. Payne, and S.D. Emr. 1997a. The AP-3 adaptor complex is essential for cargo-selective transport to the yeast vacuole. *Cell.* 91:109–118. https://doi.org/10.1016/S0092-8674(01)80013-1

Cowles, C.R., W.B. Snyder, C.G. Burd, and S.D. Emr. 1997b. Novel Golgi to vacuole delivery pathway in yeast: identification of a sorting determinant and required transport component. *EMBO J.* 16:2769–2782. https://doi.org/10.1093/emboj/16.10.2769

Cyert, M.S.. 2003. Calcineurin signaling in Saccharomyces cerevisiae: how yeast go crazy in response to stress. *Biochem. Biophys. Res. Commun.* 311:1143–1150. https://doi.org/10.1016/S0006-291X(03)01552-3

Cyert, M.S., and J. Thorner. 1992. Regulatory subunit (CNB1 gene product) of yeast Ca2+/calmodulin-dependent phosphoprotein phosphatases is required for adaptation to pheromone. *Mol. Cell. Biol.* 12:3460–3469. https://doi.org/10.1128/MCB.12.8.3460

Dunn, R., D.A. Klos, A.S. Adler, and L. Hicke. 2004. The C2 domain of the Rsp5 ubiquitin ligase binds membrane phosphoinositides and directs ubiquitination of endosomal cargo. *J. Cell Biol.* 165:135–144. https://doi.org/10.1083/jcb.200309026

Feilotter, H.E., G.J. Hannon, C.J. Ruddell, and D. Beach. 1994. Construction of an improved host strain for two hybrid screening. *Nucleic Acids Res.* 22:1502–1503. https://doi.org/10.1093/nar/22.8.1502

Garrett-Engele, P., B. Moilanen, and M.S. Cyert. 1995. Calcineurin, the Ca2+/calmodulin-dependent protein phosphatase, is essential in yeast mutants with cell integrity defects and in mutants that lack a functional vacuolar H(+)-ATPase. *Mol. Cell. Biol.* 15:4103–4114. https://doi.org/10.1128/MCB.15.8.4103

Gupta, R., B. Kus, C. Fladd, J. Wasmuth, R. Tonikian, S. Sidhu, N.J. Krogan, J. Parkinson, and D. Rotin. 2007. Ubiquitination screen using protein microarrays for comprehensive identification of Rsp5 substrates in yeast. *Mol. Syst. Biol.* 3:116. https://doi.org/10.1038/msb4100159

Imai, K., Y. Noda, H. Adachi, and K. Yoda. 2005. A novel endoplasmic reticulum membrane protein Rcr1 regulates chitin deposition in the cell wall of Saccharomyces cerevisiae. *J. Biol. Chem.* 280:8275–8284. https://doi.org/10.1074/jbc.M409428200

Justice, E.D., S.J. Barnum, and T. Kidd. 2017. The WAGR syndrome gene PRRG4 is a functional homologue of the commissureless axon guidance gene. *PLoS Genet.* 13. e1006865. https://doi.org/10.1371/journal.pgen.1006865

Klis, F.M.. 1994. Review: cell wall assembly in yeast. *Yeast.* 10:851–869. https://doi.org/10.1002/yea.320100702

Kota, J., C.F. Gilstring, and P.O. Ljungdahl. 2007a. Membrane chaperone Shr3 assists in folding amino acid permeases preventing precocious ERAD. *J. Cell Biol.* 176:617–628. https://doi.org/10.1083/jcb.200612100

Kota, J., M. Melin-Larsson, P.O. Ljungdahl, and H. Forsberg. 2007b. Ssh4, Rcr2 and Rcr1 affect plasma membrane transporter activity in Saccharomyces cerevisiae. *Genetics.* 175:1681–1694. https://doi.org/10.1534/genetics.106.069716

Lauwers, E., C. Jacob, and B. André. 2009. K63-linked ubiquitin chains as a specific signal for protein sorting into the multivesicular body pathway. *J. Cell Biol.* 185:493–502. https://doi.org/10.1083/jcb.200810114

Léon, S., Z. Erpapazoglou, and R. Haguenauer-Tsapis. 2008. Ear1p and Ssh4p are new adaptors of the ubiquitin ligase Rsp5p for cargo ubiquitylation and sorting at multivesicular bodies. *Mol. Biol. Cell.* 19:2379–2388. https://doi.org/10.1091/mbc.e08-01-0068

Levin, D.E.. 2005. Cell wall integrity signaling in Saccharomyces cerevisiae. *Microbiol. Mol. Biol. Rev.* 69:262–291. https://doi.org/10.1128/MMBR.69.2.262-291.2005

Li, M., T. Koshi, and S.D. Emr. 2015a. Membrane-anchored ubiquitin ligase complex is required for the turnover of lysosomal membrane proteins. *J. Cell Biol.* 211:639–652. https://doi.org/10.1083/jcb.201505062

Li, M., Y. Rong, Y.S. Chuang, D. Peng, and S.D. Emr. 2015b. Ubiquitin-dependent lysosomal membrane protein sorting and degradation. *Mol. Cell.* 57:467–478. https://doi.org/10.1016/j.molcel.2014.12.012

Lin, C.H., J.A. MacGurn, T. Chu, C.J. Stefan, and S.D. Emr. 2008. Arrestin-related ubiquitin-ligase adaptors regulate endocytosis and protein turnover at the cell surface. *Cell.* 135:714–725. https://doi.org/10.1016/j.cell.2008.09.025

Longtine, M.S., A. McKenzie, III, D.J. Demarini, N.G. Shah, A. Wach, A. Brachat, P. Philippsen, and J.R. Pringle. 1998. Additional modules for versatile and economical PCR-based gene deletion and modification in Saccharomyces cerevisiae. *Yeast.* 14:953–961. https://doi.org/10.1002/(SICI)1097-0061(199807)14:10<953::AID-YEA293>3.0.CO;2-U

Luo, Y., X. Liu, Y. Liu, Y. Han, and J. Li. 2019. Exogenous Calcium Ions Enhance Patulin Adsorption Capability of *Saccharomyces cerevisiae*. *J. Food Prot.* 82:1390–1397. https://doi.org/10.4315/0362-028X.JFP-18-496

MacDonald, C., S.B. Shields, C.A. Williams, S. Winistorfer, and R.C. Piper. 2020. A Cycle of Ubiquitination Regulates Adaptor Function of the Nedd4-Family Ubiquitin Ligase Rsp5. *Curr. Biol.* 30:465–479. https://doi.org/10.1016/j.cub.2019.11.086

Manford, A.G., C.J. Stefan, H.L. Yuan, J.A. Macgurn, and S.D. Emr. 2012. ER-to-plasma membrane tethering proteins regulate cell signaling and ER morphology. *Dev. Cell.* 23:1129–1140. https://doi.org/10.1016/j.devcel.2012.11.004

Marton, M.J., J.L. DeRisi, H.A. Bennett, V.R. Iyer, M.R. Meyer, C.J. Roberts, R. Stoughton, J. Burchard, D. Slade, H. Dai, et al. 1998. Drug target validation and identification of secondary drug target effects using DNA microarrays. *Nat. Med.* 4:1293–1301. https://doi.org/10.1038/3282

Mazur, P., N. Morin, W. Baginsky, M. el-Sherbeini, J.A. Clemas, J.B. Nielsen, and F. Foor. 1995. Differential expression and function of two homologous subunits of yeast 1,3-beta-D-glucan synthase. *Mol. Cell. Biol.* 15:5671–5681. https://doi.org/10.1128/MCB.15.10.5671

Munro, C.A.. 2013. Chitin and glucan, the yin and yang of the fungal cell wall, implications for antifungal drug discovery and therapy. *Adv. Appl. Microbiol.* 83:145–172. https://doi.org/10.1016/B978-0-12-407678-5.00004-0

Myat, A., P. Henry, V. McCabe, L. Flintoft, D. Rotin, and G. Tear. 2002. Drosophila Nedd4, a ubiquitin ligase, is recruited by Commissureless to control cell surface levels of the roundabout receptor. *Neuron.* 35:447–459. https://doi.org/10.1016/S0896-6273(02)00795-X

Piao, H.L., I.M. Machado, and G.S. Payne. 2007. NPFXD-mediated endocytosis is required for polarity and function of a yeast cell wall stress sensor. *Mol. Biol. Cell.* 18:57–65. https://doi.org/10.1091/mbc.e06-08-0721

Radivojac, P., V. Vacic, C. Haynes, R.R. Cocklin, A. Mohan, J.W. Heyen, M.G. Goebl, and L.M. Iakoucheva. 2010. Identification, analysis, and prediction of protein ubiquitination sites. *Proteins.* 78:365–380. https://doi.org/10.1002/prot.22555

Ritz, A.M., M. Trautwein, F. Grassinger, and A. Spang. 2014. The prion-like domain in the exomer-dependent cargo Pin2 serves as a trans-Golgi retention motif. *Cell Rep.* 7:249–260. https://doi.org/10.1016/j.celrep.2014.02.026

Rotin, D., and S. Kumar. 2009. Physiological functions of the HECT family of ubiquitin ligases. *Nat. Rev. Mol. Cell Biol.* 10:398–409. https://doi.org/10.1038/nrm2690

Roy, J., H. Li, P.G. Hogan, and M.S. Cyert. 2007. A conserved docking site modulates substrate affinity for calcineurin, signaling output, and in vivo function. *Mol. Cell.* 25:889–901. https://doi.org/10.1016/j.molcel.2007.02.014

Rusnak, F., and P. Mertz. 2000. Calcineurin: form and function. *Physiol. Rev.* 80:1483–1521. https://doi.org/10.1152/physrev.2000.80.4.1483

Sardana, R., L. Zhu, and S.D. Emr. 2019. Rsp5 Ubiquitin ligase-mediated quality control system clears membrane proteins mistargeted to the vacuole membrane. *J. Cell Biol.* 218:234–250. https://doi.org/10.1083/jcb.201806094

Scott, P.M., P.S. Bilodeau, O. Zhdankina, S.C. Winistorfer, M.J. Hauglund, M.M. Allaman, W.R. Kearney, A.D. Robertson, A.L. Boman, and R.C. Piper. 2004. GGA proteins bind ubiquitin to facilitate sorting at the trans-Golgi network. *Nat. Cell Biol.* 6:252–259. https://doi.org/10.1038/ncb1107

Shaw, J.A., P.C. Mol, B. Bowers, S.J. Silverman, M.H. Valdivieso, A. Durán, and E. Cabib. 1991. The function of chitin synthases 2 and 3 in the Saccharomyces cerevisiae cell cycle. *J. Cell Biol.* 114:111–123. https://doi.org/10.1083/jcb.114.1.111

Smoyer, C.J., S.S. Katta, J.M. Gardner, L. Stoltz, S. McCroskey, W.D. Bradford, M. McClain, S.E. Smith, B.D. Slaughter, J.R. Unruh, et al. 2016. Analysis of membrane proteins localizing to the inner nuclear envelope in living cells. *J. Cell Biol.* 215:575–590. https://doi.org/10.1083/jcb.201607043

Spang, A.. 2015. The Road not Taken: Less Traveled Roads from the TGN to the Plasma Membrane. *Membranes (Basel).* 5:84–98. https://doi.org/10.3390/membranes5010084

Stathopoulos, A.M., and M.S. Cyert. 1997. Calcineurin acts through the CRZ1/TCN1-encoded transcription factor to regulate gene expression in yeast. *Genes Dev*. 11:3432–3444. https://doi.org/10.1101/gad.11.24.3432

Stie, J., and D. Fox. 2008. Calcineurin regulation in fungi and beyond. *Eukaryot. Cell*. 7:177–186. https://doi.org/10.1128/EC.00326-07

Tatjer, L., A. González, A. Serra-Cardona, A. Barceló, A. Casamayor, and J. Ariño. 2016. The Saccharomyces cerevisiae Ptc1 protein phosphatase attenuates G2-M cell cycle blockage caused by activation of the cell wall integrity pathway. *Mol. Microbiol*. 101:671–687. https://doi.org/10.1111/mmi.13416

Tharanathan, R.N., and F.S. Kittur. 2003. Chitin--the undisputed biomolecule of great potential. *Crit. Rev. Food Sci. Nutr*. 43:61–87. https://doi.org/10.1080/10408690390826455

Weiskoff, A.M., and J.C. Fromme. 2014. Distinct N-terminal regions of the exomer secretory vesicle cargo Chs3 regulate its trafficking itinerary. *Front. Cell Dev. Biol*. 2:47. https://doi.org/10.3389/fcell.2014.00047

Yoshimoto, H., K. Saltsman, A.P. Gasch, H.X. Li, N. Ogawa, D. Botstein, P.O. Brown, and M.S. Cyert. 2002. Genome-wide analysis of gene expression regulated by the calcineurin/Crz1p signaling pathway in Saccharomyces cerevisiae. *J. Biol. Chem*. 277:31079–31088. https://doi.org/10.1074/jbc.M202718200

Zhu, L., J.R. Jorgensen, M. Li, Y.S. Chuang, and S.D. Emr. 2017. ESCRTs function directly on the lysosome membrane to downregulate ubiquitinated lysosomal membrane proteins. *eLife*. 6. e26403. https://doi.org/10.7554/eLife.26403

## Supplemental material


https://doi.org/10.1083/jcb.201909158

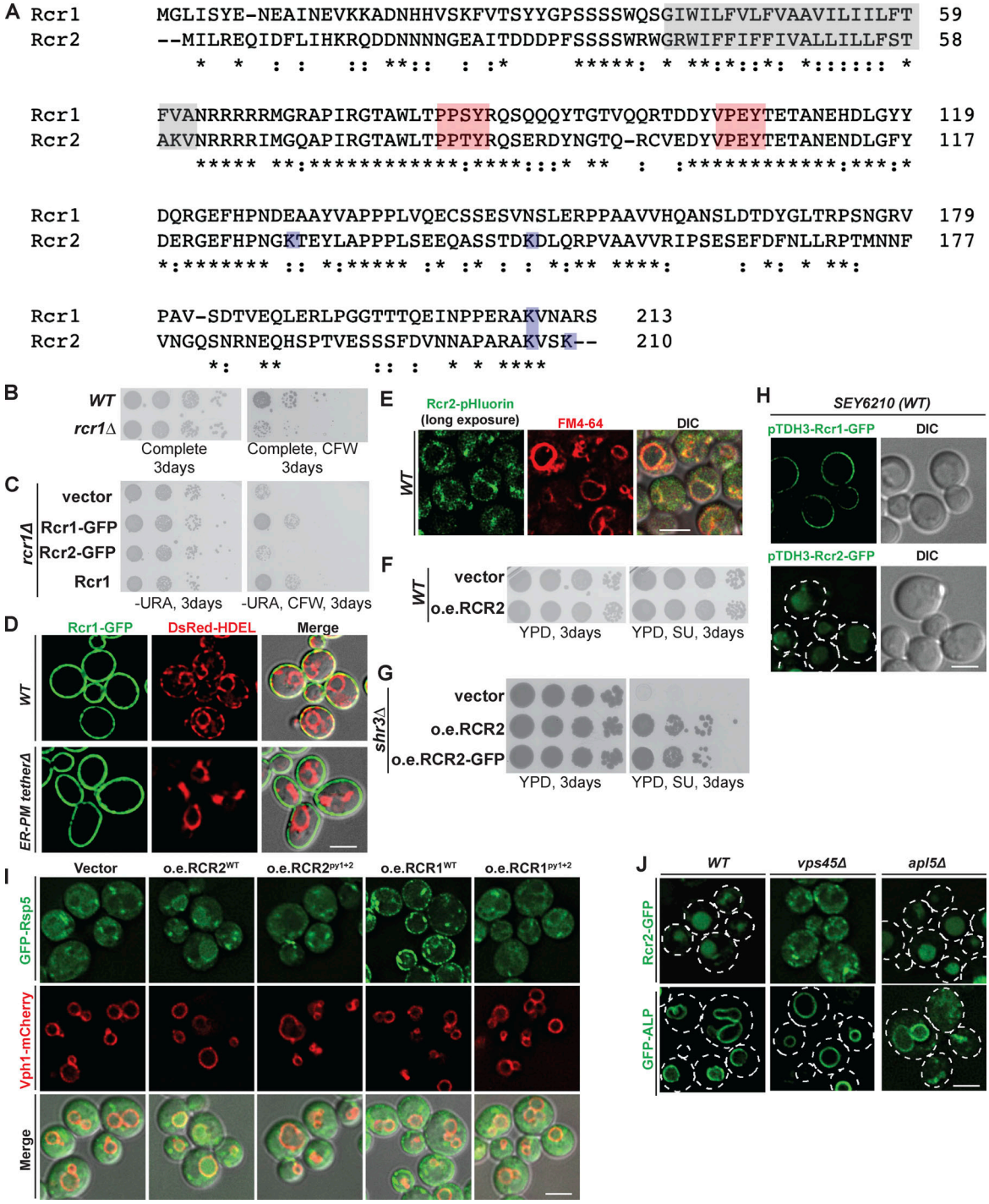


Figure S1. **Recruitment of Rsp5 to different subcellular localizations by Rcr1 and Rcr2. (A)** Amino acids sequence alignment between Rcr1 and Rcr2. Symbol (*) represents the identical residues, and symbol (:) stands for the similar residues. The gray shaded region represents the transmembrane domain of Rcr1 and Rcr2 proteins, predicted by TMHMM server 2.0. The red shaded residues are the PY-motifs of Rcr1 and Rcr2. The blue shaded residues stand for cytosolic lysines of Rcr1 and Rcr2. **(B)** Mild CFW sensitivity of rcr1Δ mutant. Cell growth assay of rcr1Δ cells grown at 30°C for 3 d in the presence or absence of CFW (150 µg/ml). **(C)** Rcr1-GFP is functional. Cell growth assay of rcr1Δ cells grown at 30°C for 3 d on the SCD-Uracil plate in the presence or absence of CFW (150 µg/ml) bearing empty vector, Rcr1-GFP, Rcr2-GFP, and non-tagged Rcr1 expression vectors. **(D)** Rcr1 is not an ER membrane protein. Localization of Rcr1-GFP and DsRed-HDEL within WT and the ER-PM tetherΔ mutant. **(E)** Localization of Rcr2-pHluorin and FM4-64 in WT cells. **(F)** WT cells are SU-resistant. Cell growth assay of WT cells at 30°C for 3 d on YPD plate with or without SU (100 µg/ml) bearing empty vector, r overexpressing (o.e.) RCR2 expression vector. **(G)** Rcr2-GFP is functional. Cell growth assay of shr3Δ mutant at 30°C for 3 d on YPD plate with or without SU (100 µg/ml) bearing empty vector, o.e. RCR2, or o.e. RCR2-GFP expression vectors. **(H)** Analysis of Rcr1-GFP and Rcr2-GFP under the pTDH3 promoter. In WT cells, fluorescence microscopy of Rcr1-GFP and Rcr2-GFP expressed from the pTDH3 promoter. **(I)** Recruitment of Rsp5 to different subcellular localizations by Rcr1 and Rcr2. Fluorescence microscopy of GFP-Rsp5 recruitment to the vacuole or PM upon overexpression of o.e. $RCR2^{WT}$, o.e. $RCR2^{py1+2}$, o.e. $RCR1^{WT}$ or o.e. $RCR1^{py1+2}$. **(J)** Rcr2 is sorted to the vacuole via the VPS-pathway. Fluorescence microscopy of Rcr1-GFP and GFP-ALP in WT, vps45Δ mutant or apl5Δ mutant. Scale bars, 2 µm.

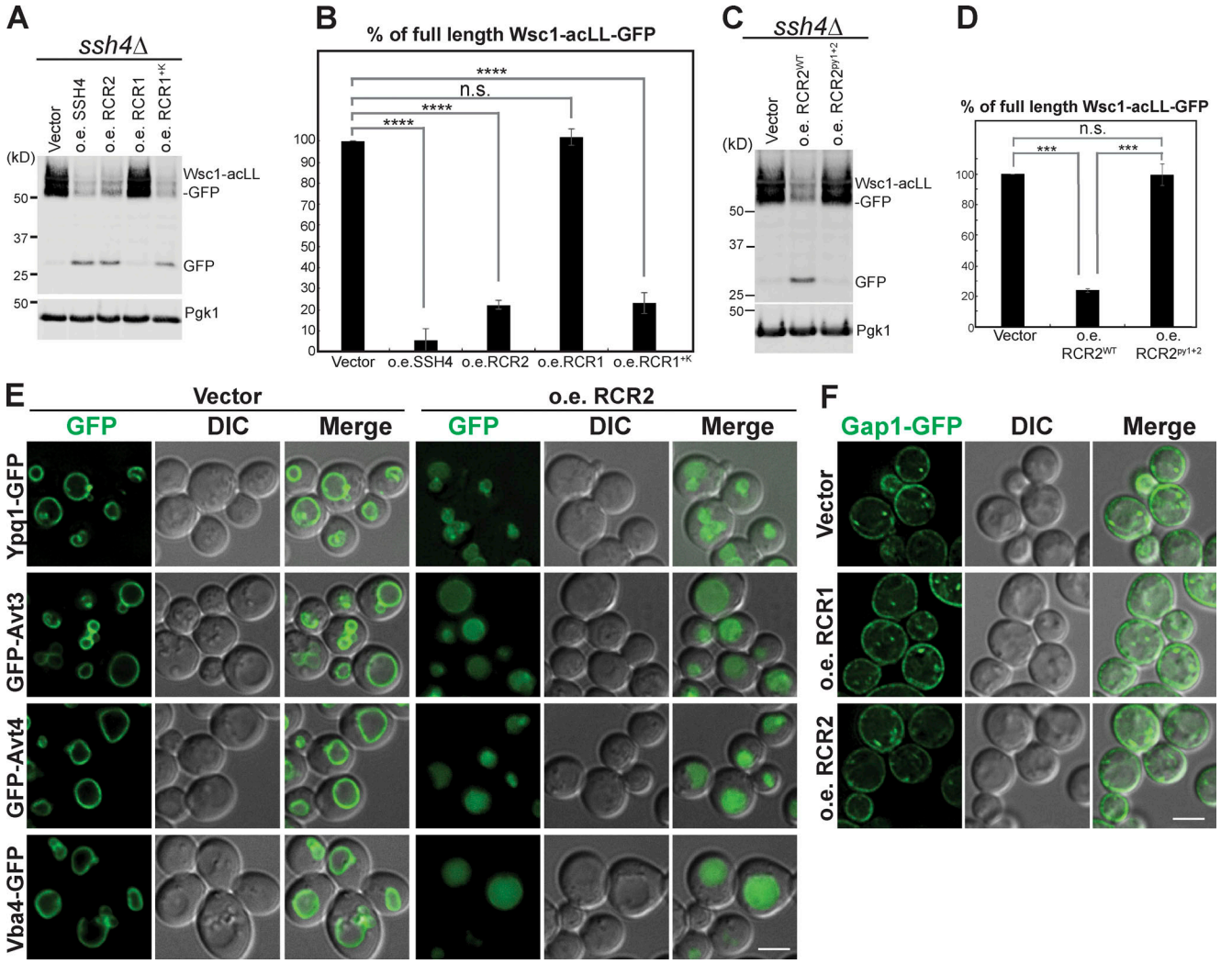


Figure S2. **Down-regulation of vacuole membrane proteins upon Rcr2 overexpression. (A)** Western blot analysis of WaG in the ssh4Δ mutant bearing an empty vector, or with overexpression of SSH4, RCR2, RCR1, and RCR1$^{+K}$. The blot was probed with GFP and Pgk1 antibodies. **(B)** Quantification analysis of full-length WaG in the experiment (A). **(C)** Western blot analysis of WaG in the ssh4Δ mutant with an empty vector, or overexpression of RCR2$^{WT}$ or RCR2$^{py1+2}$ mutant. The blot was probed with GFP and G6PDH antibodies. **(D)** Quantification of the Western blot analysis of WaG in C. **(E)** Fluorescence microscopy of vacuole membrane proteins Ypq1-GFP, GFP-Avt3, GFP-Avt4, and Vba4-GFP in the WT cells bearing control or RCR2 overexpression vector. **(F)** Gap1-GFP localization in WT cells bearing control, RCR1, or RCR2 overexpression vectors. The Gap1-GFP expression was induced by switching from ammonium-containing medium to poor-nitrogen medium for 1 h. The comparison of "% of full length WaG" between vector, o.e. SSH4, o.e. RCR2, o.e. RCR1, o.e. RCR1$^{+K}$, and o.e. RCR2$^{py1+2}$ was analyzed by two-tailed *t* test. P, < 0.0001, α = 0.05 (Bonferroni correction), *n* = 3. Scale bars, 2 µm.

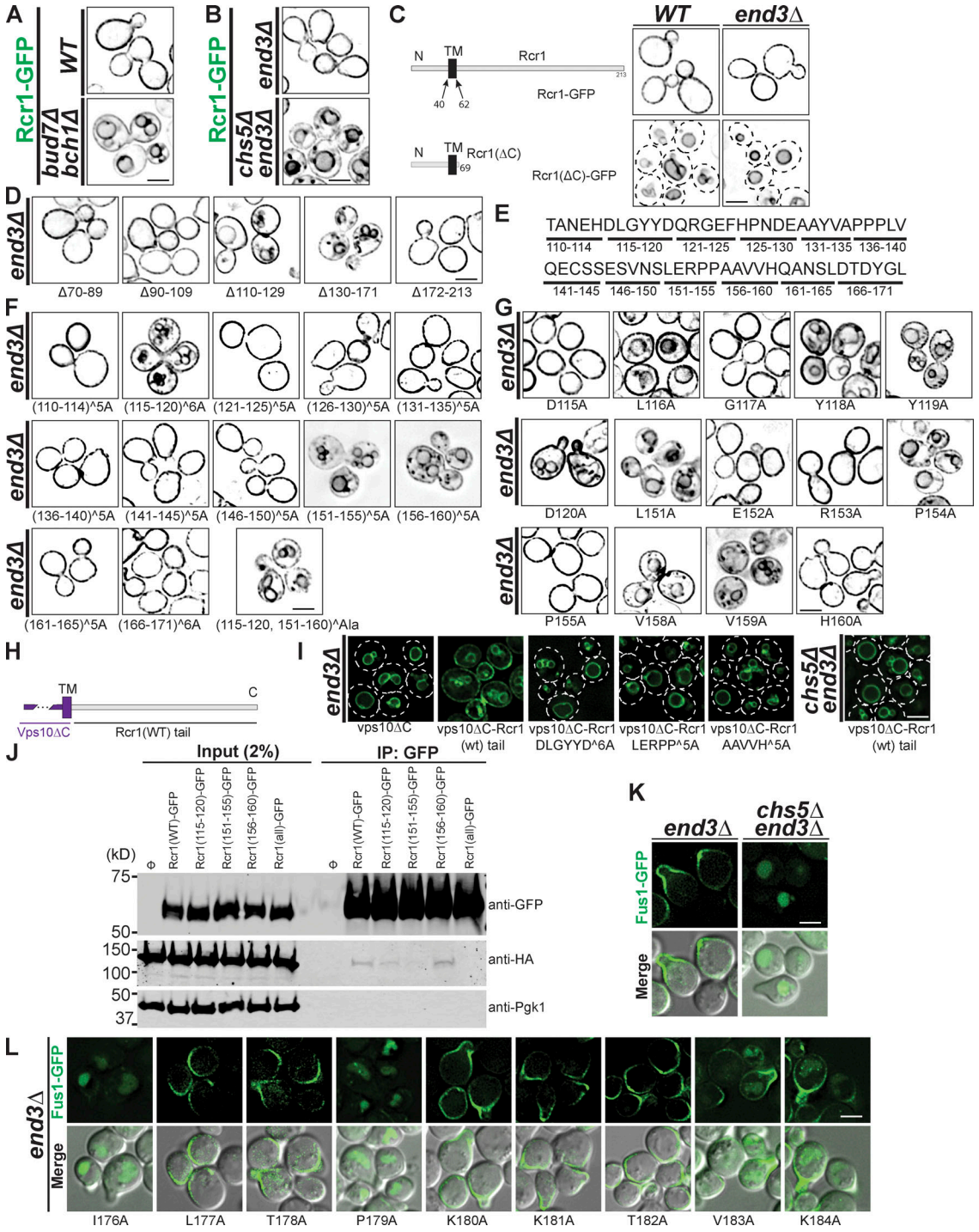


Figure S3. **The plasma membrane sorting signal within the Rcr1 cytosolic tail. (A)** Localization of Rcr1-GFP in the ChAPs mutant bud7Δbch1Δ. **(B)** Localization of Rcr1-GFP in end3Δ and chs5Δend3Δ mutants. **(C)** Localization of WT and a C-terminal truncation of Rcr1-GFP in both WT and end3Δ mutant. **(D)** Localization of Rcr1-GFP tail truncation mutants expressed in an end3Δ strain: Δ70–89, Δ90–109, Δ110–129, Δ130–171, and Δ172–213. **(E)** Amino acids sequence of Rcr1 (110–171). **(F)** Fluorescence microscopy of Rcr1-GFP alanine scanning mutants within the region 110–171 of the Rcr1 C-tail: (110–114)^5A, (115–120)^6A, (121–125)^5A, (126–130)^5A, (131–135)^5A, (136–140)^5A, (141–145)^5A, (146–150)^5A, (151–155)^5A, (156–160)^5A, (161–165)^5A, (166–171)^5A and (115–120, 151–160)^Ala in end3Δ mutant. **(G)** Localization of Rcr1 single alanine substitution mutants within the bipartite sorting motifs: D115A, L116A, G117A, Y118A, Y119A, D120A, L151A, E152A, R153A, P154A, P155A, V158A, V159A, and H160A in end3Δ mutant. **(H)** A schematic of chimeric protein Vps10(ΔC)-Rcr1. **(I)** Fluorescence microscopy analysis of Vps10(ΔC)-fusion proteins with the indicated Rcr1 tail mutants, in either end3Δ or end3Δchs5Δ. Quantifications of figures D, F, G, and I are shown in Fig. 2 B–D and G, respectively. **(J)** IP of the indicated Rcr1-GFP mutants and blotting for co-IPed Chs5-3HA. **(K)** Localization of Fus1-GFP in end3Δ and chs5Δend3Δ mutants. The mutant cells bearing Fus1-GFP vector were grown in synthetic medium to mid-log phase (OD 600 reaches around 0.4) and treated with 50 ng/ml α-factor pheromone peptide for 90 min, fixed with formaldehyde, and washed with water twice before fluorescence microscopy. **(L)** Localization of Fus1 single alanine substitution mutants in end3Δ mutant: I176A, L177A, T178A, P179A, K180A, K181A, T182A, V183A, and K184A. Scale bars, 2 µm.

**Table S1 is provided online as a separate Excel file. Table S1 lists strains and plasmids used in this study.**